Temperature fluctuations and heat transport in the edge regions of a tokamak

P. C. Liewer, J. M. McChesney, S. J. Zweben,[a] and R. W. Gould
Department of Applied Physics, California Institute of Technology, Pasadena, California 91125

(Received 22 March 1985; accepted 8 September 1985)

Electron temperature fluctuations have been investigated in the edge region of the Caltech research tokamak [S. J. Zweben and R. W. Gould, Nucl. Fusion **25**, 171 (1985)], and an upper limit to this fluctuation level was found at $\tilde{T}_e/T_e \lesssim 15\%$. This measurement, together with previous measurements of density and electric and magnetic field fluctuations, allows a unique comparison of the heat transport resulting from three basic turbulent mechanisms: (1) heat flux from the particle flux resulting from microscopic density and electric field fluctuations; (2) thermal conduction resulting from microscopic temperature and electric field fluctuations; and (3) thermal conduction resulting from microscopic magnetic field fluctuations. The measurements indicate that, in the edge regions, the electron heat transport caused by the measured turbulence-induced particle flux is comparable to or greater than that caused by the thermal conduction associated with the electron temperature and electric field fluctuations, and is significantly greater than that resulting from the measured magnetic fluctuations. This electron heat loss caused by the plasma turbulence is found to be an important electron energy loss mechanism in the edge regions.

I. INTRODUCTION AND SUMMARY

Extensive measurements have been made of the microscopic fluctuations in tokamak plasmas because of their possible role in causing the observed anomalous energy transport.[1] Broadband density fluctuations have been measured in the central and edge regions of several large tokamaks, including PLT,[2] Alcator A and C,[3] TFR,[4] PDX,[5] and TEXT,[6] using electromagnetic wave scattering techniques. However, measurements of the density fluctuations alone are not sufficient to determine the "anomalous" transport associated with these fluctuations.

In the cooler edge regions, where probes can be used, direct measurements of the radial particle transport caused by microscopic density and electric field fluctuations have been made by correlating the fluctuations in the density ($\tilde{n}$) and the poloidal electric field ($\tilde{E}_p$).[7-10] For low-frequency fluctuations, the contribution to the radial particle flux from the density and electric field fluctuations is given by the correlation of the density fluctuations with the radial velocity fluctuations, $\tilde{V}_r = c\tilde{E}_p/B$, i.e., $\Gamma_r(\tilde{E}) = c\langle \tilde{n}\tilde{E}_p \rangle/B$, where B is the toroidal magnetic field strength. The particle flux has been found to be large and outward in tokamaks where this measurement has been made.[7-10] However, to learn about heat conduction, knowledge of the pressure or temperature fluctuations is also needed.

In this paper, results are presented from an investigation of the electron temperature fluctuations in the edge regions of the Caltech Research Tokamak.[10] Using a swept Langmuir probe, an upper bound on the possible electron temperature fluctuations was established at $0 < |\tilde{T}_e/T_e| < 15\%$. Simultaneous measurements showed density and floating potential fluctuation levels of $\tilde{n}/n \sim e\tilde{\phi}/T_e \sim 30\%$–$50\%$.

It is also shown here that, in the edge regions, the expression for the electron heat flux from thermal conduction caused by low-frequency electrostatic fluctuations is $q_r(\tilde{E}) \cong (5/2)nc\langle \tilde{T}_e\tilde{E}_p \rangle/B$. Using this expression and the measured upper bound on the electron temperature fluctuations, an upper bound has been determined for this electron heat loss by thermal conduction. This result, together with previous measurements[7,10,11] in the edge regions of the Caltech tokamak, makes possible a unique comparison of this conductive heat transport to the electron heat transport resulting from two other turbulent mechanisms: (1) heat transport caused by the measured fluctuation-induced particle flux $[(5/2)T_e\Gamma_r(\tilde{E}) = (5/2)T_e c\langle \tilde{n}\tilde{E}_p \rangle/B\,]$ and (2) thermal conduction resulting from the microscopic stochastic magnetic field fluctuations $[q_r(\tilde{B}) \cong K_e(\tilde{B})dT_e/dr$, where $K_e(\tilde{B})$ is a model-dependent anomalous thermal conductivity resulting from the magnetic field fluctuations].

This comparison indicates that the electron heat loss caused by the fluctuation-induced particle flux may be as large as or larger than the loss from thermal conduction resulting from the temperature and electric field fluctuations, assuming the turbulence is poloidally symmetric. Moreover, the heat loss from the fluctuation-induced particle flux is estimated to be about 100 times larger than the loss from thermal conduction resulting from stochastic magnetic field fluctuations calculated using the measured $\tilde{B}$ level and the Rechester and Rosenbluth collisionless model for the thermal conductivity $K_e(\tilde{B})$.[12]

The particle diffusion coefficient in the edge region, estimated from the measured $\tilde{E}$-induced particle flux, is $D(\tilde{E}) = \Gamma_x/(dn/dr) \sim 1$–$2 \times 10^5$ cm^2/sec. This is somewhat larger than the global electron thermal diffusivity of $\chi_e \sim 0.5$–1.0×10^5 cm^2/sec estimated from the measured global energy confinement time of 0.5–1.0 msec using the formula $\chi_e \sim a^2/4\tau_E$. Thus the energy lost through this anomalous particle diffusion is an important electron energy loss mechanism in the edge regions of this tokamak.

[a] Present address: Princeton Plasma Physics Laboratory, Princeton, New Jersey 08544.

 0031-9171/86/010309-09$01.90

The outline of this paper is as follows. In Sec. II, the expression for the heat flux associated with fluctuations in electron temperature and electric field is derived. The measurement of the upper limit to electron temperature fluctuations is presented in Sec. III. In Sec. IV, the magnitudes of the turbulent heat fluxes and diffusivities are estimated using measured values for the fluctuations. The results are discussed in Sec. V.

II. EXPRESSIONS FOR PARTICLE AND HEAT FLUXES RESULTING FROM ELECTROSTATIC FLUCTUATIONS

To determine the anomalous transport resulting from observed microscopic fluctuations, expressions are needed that relate the particle and heat fluxes to the various fluctuations. The expression for the radial particle flux resulting from electrostatic fluctuations is well known [see, e.g., Refs. (13)–(16)]:

$$\Gamma_r = (c/B)\langle \tilde{n}\tilde{E}_p \rangle, \tag{1}$$

where $\tilde{n}$ is the density fluctuation, $\tilde{E}_p$ is the poloidal electric field fluctuation, and $\langle\ \rangle$ denotes a time average over the fluctuation time scale so that $\langle \tilde{n} \rangle = \langle \tilde{\mathbf{E}} \rangle = 0$, but the correlation $\langle \tilde{n}\tilde{\mathbf{E}} \rangle$ can be finite. Here, we present a simple expression for the electron heat flux caused by the fluctuations in electron temperature and poloidal electric field valid for the edge regions of the Caltech tokamak.

The transport equations for a tokamak plasma can be written as

$$\frac{\partial}{\partial t} n + \frac{\partial}{\partial x} \Gamma_x = S_n,$$

$$\frac{3}{2}\frac{\partial}{\partial t} nT + \frac{\partial}{\partial x}\left(\frac{5}{2} TnV_x + q_x\right) = V_x \frac{\partial nT}{\partial x} + S_T, \tag{2}$$

where S_n and S_T are particle and heat source terms, respectively, and, where, for simplicity, slab geometry has been used with $\hat{x}$ corresponding to the radial direction, $\hat{z}$ corresponding to the toroidal direction, and $\hat{y}$ corresponding to the poloidal direction (so $\tilde{E}_y \equiv \tilde{E}_p$ throughout). In the presence of turbulence, the various fluid quantities are defined in terms of the time-averaged distribution function $\langle F \rangle$:

$$n = \int_{-\infty}^{\infty} d\mathbf{v} \langle F \rangle,$$

$$\frac{3}{2} nT = \frac{3}{2} p = \frac{1}{2} \int_{-\infty}^{\infty} d\mathbf{v}\, m(v - V)^2 \langle F \rangle, \tag{3}$$

$$\Gamma_x = nV_x = \int_{-\infty}^{\infty} d\mathbf{v}\, v_x \langle F \rangle,$$

and

$$q_x = \frac{1}{2} \int_{-\infty}^{\infty} d\mathbf{v}(v_x - V_x) m(v - V)^2 \langle F \rangle. \tag{4}$$

The pressure has been assumed to be isotropic. Here Γ_x is the particle flux and q_x is the heat flux attributed to thermal conduction. It can be seen that the heat flux caused by the particle flux is $(5/2)T\Gamma_x$. These fluxes will, in general, contain contributions from both classical and turbulent (anomalous) processes.

Expressions for the contribution to these fluxes from low-frequency ($\omega \ll \omega_{ci}$), electrostatic ($\tilde{B} = 0$) turbulence have been calculated by several authors[13–16]; the particle flux was given in Eq. (1). To obtain an expression for the conductive heat flux q_x, we start with the following expression for the total energy flux W_x resulting from electrostatic turbulence:

$$W_x = \frac{1}{2} \int d\mathbf{v}\, mv^2 v_x \langle F \rangle$$

$$= \frac{c}{B}\left(\langle \tilde{\epsilon}\tilde{E}_y \rangle + \left\langle \int d\mathbf{v}\, mv_y \mathbf{v}\cdot\tilde{\mathbf{E}}\tilde{F} \right\rangle \right). \tag{5}$$

A derivation of W_x, as well as Γ_x, is given in the Appendix and in Ref. 16. Here $\tilde{F}$ is the fluctuation in the distribution function caused by the turbulence, and $\tilde{n}$ and $\tilde{\epsilon}$ as well as other microscopic (fluctuating) quantities are defined as follows:

$$\tilde{n} = \int d\mathbf{v}\, \tilde{F}, \quad n\tilde{\mathbf{V}} = \int d\mathbf{v}\, \mathbf{v}\tilde{F},$$

$$\tilde{\epsilon} = \frac{1}{2} \int d\mathbf{v}\, mv^2 \tilde{F},$$

$$\frac{3}{2}\tilde{p} = \frac{1}{2} \int d\mathbf{v}\, m(v - V)^2 \tilde{F}, \tag{6}$$

$$\tilde{T} = (\tilde{p} - T\tilde{n})/n,$$

where the fluctuations in energy, density, and velocity are related via

$$\tilde{\epsilon} = \tfrac{3}{2}\tilde{p} + mn\mathbf{V}\cdot\tilde{\mathbf{V}} - \tfrac{1}{2}\tilde{n}mV^2.$$

Note that we have included separate definitions of $\tilde{p}$ and $\tilde{T}$ so that the contribution to the pressure fluctuations resulting from density fluctuations ($\tilde{n}T$) is clearly separated from the contribution resulting from temperature fluctuations ($n\tilde{T}$). Thus, using our definitions, a fluctuating distribution function of the form $\tilde{F} = (e\tilde{\phi}/T_e)F_M$, where $F_M = \langle F \rangle$ is a Maxwellian distribution function with (nonfluctuating) temperature T_e, produces a pressure fluctuation ($T_e\tilde{n}$) but no temperature fluctuation, consistent with the physical picture.

Using the definitions in Eqs. (3)–(5), the conductive heat flux q_x can be written in terms of the total energy flux W_x as follows:

$$q_x = W_x - V_x(mnV^2/2 + \tfrac{5}{2}p). \tag{7}$$

Up to this point, the equations for the particle and energy fluxes are valid for both electron and ions provided the assumptions in the derivation are valid (see the Appendix). No assumption of small-amplitude fluctuations has been made, and thus these expressions can be used in the edge regions of a tokamak where $\tilde{n}/n \sim 50\%$.

By specializing to the case of the electrons and taking $V^2 \ll T/m$, $\tilde{V}^2 \ll T/m$, and $V\tilde{V} \ll (T/m)(\tilde{n}/n)$, consistent with the experimental observations in tokamaks, we obtain from Eqs. (5)–(7):

$$q_x = (c/B)\langle \tfrac{3}{2}\tilde{E}_y\tilde{p} + \tilde{\mathbf{E}}\cdot\tilde{\mathbf{p}}_y - \tfrac{5}{2}T\tilde{n}\tilde{E}_y \rangle, \tag{8}$$

where $\tilde{\mathbf{p}}_y = \int d\mathbf{v}\, m(\mathbf{v} - \mathbf{V})(v_y - V_y)\tilde{F}$ and all quantities now refer to electrons.

For the turbulence in the edge regions of a tokamak, where the frequency of the fluctuations is low compared to

the electron–electron collision time, one can approximate the electron pressure fluctuations as isotropic with $\tilde{\mathbf{p}}_y = \tilde{p}\hat{y}$. With this approximation, the expression for the electron conductive heat flux in Eq. (8) becomes

$$q_x \cong \tfrac{5}{2}(c/B)\langle \tilde{E}_y(\tilde{p} - T\tilde{n})\rangle = \tfrac{5}{2}(c/B)n\langle \tilde{T}\tilde{E}_y\rangle. \quad (9)$$

Thus the conductive electron heat flux caused by low-frequency, electrostatic turbulence depends on the correlation of the temperature and electric field fluctuations. Note that, in this limit, the total electron thermal energy flux Q_x can be written as $Q_x \equiv (5/2)T\Gamma_x + q_x = (5/2)c\langle \tilde{p}\tilde{E}_y\rangle/B$. Equations for the heat fluxes in the more general case of anisotropic pressure fluctuations can be found in the work of Krall and McBride.[15]

III. MEASUREMENT OF ELECTRON TEMPERATURE FLUCTUATIONS

A. Method of measurement

The basic parameters of the Caltech tokamak are shown in Table I. In the present work, we will be concerned only with the edge plasma, i.e., $0.75 < r/a < 1.0$. In this region the electron density is approximately $5\times10^{11} - 10^{12}$ cm^{-3} and the electron temperature is approximately 10–30 eV.[17] It is important to note that the edge plasma parameters in this small tokamak are similar to the edge parameters of the larger tokamaks,[18] and also that turbulence properties of the edge density are similar to those of larger tokamaks.[17] Thus it is plausible that the $\tilde{T}_e$ measurements presented here are relevant for tokamak edge plasmas in general.

The plasma electron temperature is conventionally measured by sweeping the applied voltage V to a single Langmuir probe and monitoring the collected current I.[18,19] Assuming a Maxwellian distribution for electron energies, the collected electron current for a Langmuir probe for $V - \phi_s$ is given by[19]

$$I_e = I_{e,\mathrm{sat}} \exp[e(V - \phi_s)/kT_e], \quad (10)$$

where V is the probe voltage, ϕ_s is the plasma potential, and the electron saturation current $I_{e,\mathrm{sat}}$ for a probe of area A is given by

$$I_{e,\mathrm{sat}} = neA(kT_e/2\pi m_e)^{1/2}.$$

There is of course a corresponding, though much smaller, ion saturation current $I_{i,\mathrm{sat}}$ that must first be subtracted from the total probe current I in order to obtain the electron current of Eq. (10). By plotting the logarithm of the electron current against the probe bias V, one can determine the electron temperature from the inverse slope of the straight line fit. Generally this fit is performed over a voltage range between the floating potential ϕ_f (at which $I_e = I_{i,\mathrm{sat}}$) and the space potential ϕ_s, where these potentials are defined as usual by[19]

$$\phi_s - \phi_f = \frac{kT_e}{2e}\ln\left(\frac{\pi}{2}\frac{m_i}{m_e}\right). \quad (11)$$

TABLE I. Caltech tokamak parameters.

Major radius	R	45 cm
Minor radius	a	16 cm
Toroidal field	B	3.5 kG
Plasma current	I	25 kA
Line-averaged density	n_e	10^{12}–10^{13} cm^{-3}
Central electron temperature	$T_e(0)$	100 eV

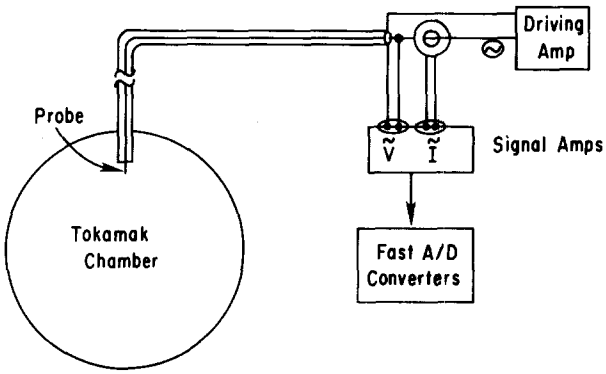

FIG. 1. Experimental layout for the swept-probe T_e measurement. The driving amplifier produced a triangular waveform with $f = 250$ kHz at $V < 150$ V. The probe current was monitored with a fast Rogowski coil. An additional variable capacitor was used to null out the displacement currents caused by cable capacitance of $\cong 100$ pF.

In order to measure the temporal fluctuations in T_e, one would like to sweep the probe voltage rapidly enough so that a complete (I,V) sweep is performed over a time scale much less than a typical period for $\tilde{T}_e$ fluctuations. Alternatively, for a sweep frequency f one can at best measure $\tilde{T}_e$ fluctuations up to a maximum frequency $f/2$ (Nyquist frequency). If in fact the variations in $\tilde{n}$ and $\tilde{\phi}$ over a sweep period are significant, there are additional uncertainties introduced into the T_e measurement (see Sec. III C).

In the present experiment, the typical frequency for $\tilde{n}$ and $\tilde{\phi}$ fluctuations is 100–200 kHz,[17] while the sweep frequency was limited by the bandwidth of the driving amplifier to at most 250 kHz; thus the sweep period was only slightly less than the time scale for changes in $\tilde{n}$ and $\tilde{\phi}$ (and presumably, in $\tilde{T}_e$). Thus this hardware limitation in sweeping speed set the main limitation on the accuracy and bandwidth of the $\tilde{T}_e$ measurement.

The Langmuir probe used had a single cylindrical tungsten tip 1 mm in diameter and 2 mm in length mounted into a 5 mm grounded stainless steel shaft and insulated from the shaft by a recessed ceramic sleeve. A second, identical electrode was mounted 3 mm away from the first in order to simultaneously monitor either the floating potential or the ion saturation current fluctuations. These probe tips were as small as possible in order to avoid probe damage caused by the melting from the normal heat load from the tokamak pulse. Note that these measurements were made with the probes located at the top of the plasma for all the data described here.

The probe voltage was swept with a specially built amplifier capable of drawing 1–2 A at a maximum probe bias of approximately 150 V with respect to ground (see Fig. 1). Near maximum current and voltage the driving amplifier's response was such that a maximum sweep frequency for an undistorted triangular voltage waveform was ~ 250 kHz.

The probe current was monitored using a commerical

Rogowski coil and fast signal amplifier with a system bandwidth of $\gtrsim 1$ MHz. A variable capacitor was introduced into the probe driving circuit to null out the probe cable capacitance. Data acquisition was facilitated by means of LeCroy 2256AS transient recorders operating at a sampling rate of 10 MHz. A difficulty with this digitization system was a small amount of memory (1K) available with these transient recorders. This precluded the storage of more than 25 complete I–V characteristics per tokamak discharge.

B. Results

Figure 2 shows a sample of the raw data obtained with the Langmuir probe swept at 250 kHz. Note that the swept current and voltage records were only 100 μsec (1024 samples) long. The electron and ion saturation currents (roughly corresponding to the upper and lower envelopes of the current sweep, respectively) give an indication of how the plasma density was varying over the duration of the data sample. Also shown in Fig. 2 is the time varying floating potential recorded during the same discharge.

Figure 3 shows three plots of $\ln(I_e)$ vs V for three typical probe sweeps. The data analysis program selected only those data points that fell on an exponential curve (filled circles). Those points that fell in the saturation regions (unfilled circles) were excluded from further analysis. A least squares fit was then performed on the selected points, and the electron temperature was found from the inverse slope of the straight line.

Two examples of the inferred temperature versus time are displayed in Fig. 4. The probe was 1.5 cm into the plasma for Fig. 4(a) and 1.0 cm into the plasma for Fig. 4(b). In the first example, the mean temperature was 19.1 eV with the rms deviation of 13%, while for the second example the mean temperature was 15.6 eV with an rms deviation of 14%. These average temperatures roughly agreed with those obtained previously with a slowly swept probe in the same edge region.[17]

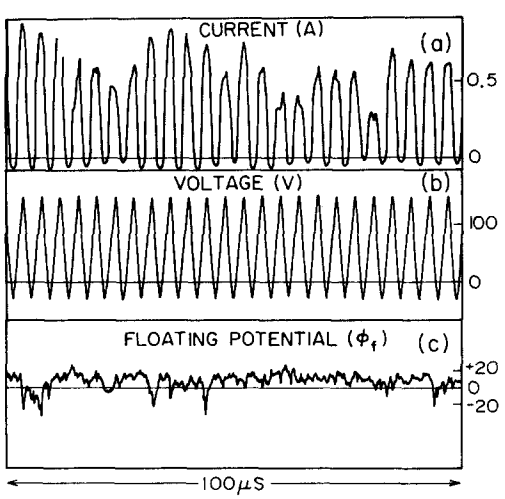

FIG. 2. Raw data on (a) probe current, (b) probe voltage, and (c) simultaneously measured $\tilde{\phi}_f$ (using a separate probe) during a typical tokamak discharge. Note that the envelope of the current trace is varying considerably from sweep-to-sweep, indicating that the density is varying on the time scale comparable to the sweeping voltage.

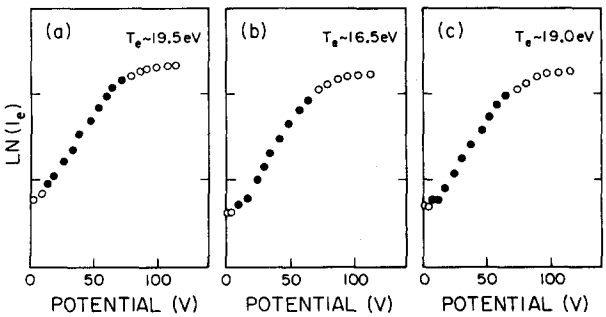

FIG. 3. Three typical ln I_e vs V plots reconstructed from swept probe data such as those shown in Fig. 2. Filled circles represent points used to calculate the electron temperature. Each point is separated by 0.1 msec in time (10 MHz digitization speed).

The evaluation of the error bars associated with the T_e points is evidently crucial for interpreting the observed variation in T_e. As discussed in Sec. III C, the major uncertainty in this T_e measurement is caused by the variations expected in $\tilde{n}$ and $\tilde{\phi}$ over the sweep period. To within the approximately $\pm$ 15% uncertainty, as indicated by typical error bars, there is no significant $\tilde{T}_e$ fluctuation detectable; that is, $\tilde{T}_e/T_e < 15\%$ is an upper bound set by these results.

Figure 5 shows simultaneous measurements of T_e, n, and ϕ_f versus time. For ease of comparison, these quantities were normalized to their average values in the case of T_e and n, and to T_e (eV) in case of ϕ_f (n was assumed to be proportional to $I_{e,\mathrm{sat}}$). No temporal correlation was found between $\tilde{T}_e$ and $\tilde{n}$ or $\tilde{\phi}_f$. It was clear that any existing temperature fluctuation level was considerably smaller than either the density or the floating potential fluctuation levels. For the data displayed in Fig. 5, the maximum possible rms tempera-

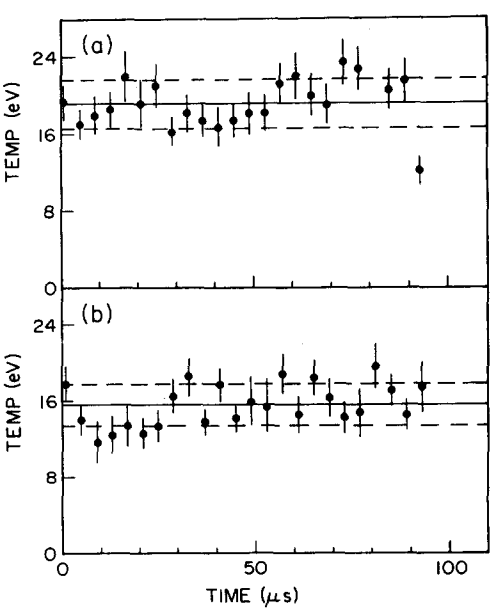

FIG. 4. Typical plots of inferred T_e versus time based on analyses similar to those shown in Fig. 3. (a) Probe position 1.5 cm into plasma and (b) probe position 1.0 cm into the plasma. The solid horizontal lines are the mean values for T_e, the dashed horizontal lines are the average rms deviations form the mean, and the vertical solid lines are the estimated uncertainties for each measurement.

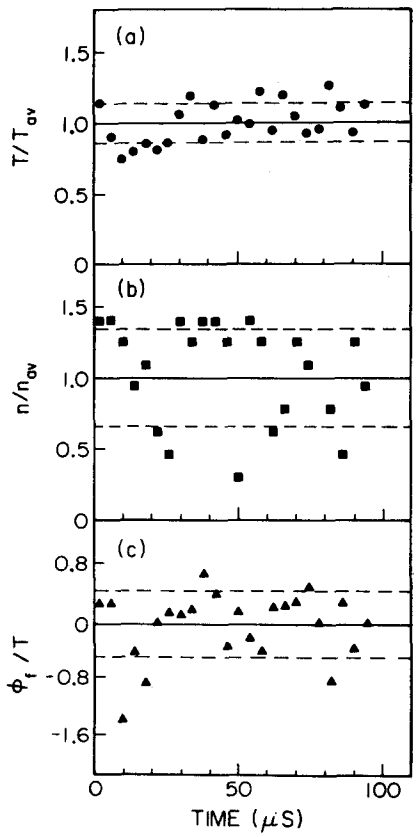

FIG. 5. Typical variations in T_e versus time compared to typical variations in n (as monitored by the variations in electron saturation current) and $\tilde{\phi}_f$ (as monitored by a separate probe). The dashed lines are the rms deviations from the mean in each case.

ture fluctuation level was 14%, while for the density data it was 34% and for the normalized floating potential data 47%.

C. Uncertainties in the $\tilde{T}_e$ measurement

Any claim as to the existence of temperature fluctuations depends on the individual T_e error bar being much less than the observed rms T_e fluctuation level. Hence it is important to explain how the error bars of Fig. 4 were derived.

There were two contributions to the error bars shown. The first resulted from the deviation of electron distribution from Maxwellian, which was reflected in the probable error in the slope of the $\ln(I_e)$ vs V curve as determined from a least-squares analysis; this error was found to be 3%–5%. The second source of error was more subtle and was caused by the implicit dependence of the slope-inferred temperature T_e' on the expected density and potential variations that occurred during the sweep. Differentiating Eq. (10) with respect to the sweep voltage V yields

$$\frac{d\ln I_e}{dV}=\frac{d\ln n}{dV}+\frac{e}{kT_e}\left(1-\frac{d\phi_s}{dV}\right), \tag{12}$$

where the actual temperature T_e was assumed constant over the sweep. Since T_e' is given by $(d\ln I_e/dV)^{-1}$, we can write

$$\frac{\Delta T_e'}{T_e}\cong\frac{kT_e}{e}\left(\frac{d\ln n}{dV}\right)-\frac{d\phi_s}{dV}, \tag{13}$$

where $d(\ln n)/dV$ is related to the average density variation expected over a voltage sweep V, and $d\phi_s/dV$ is the average space potential variation expected over the same voltage sweep. Thus variations in the slope-inferred temperature T_e' (such as those plotted in Fig. 4) can be produced by the variations of $\tilde{n}$ and/or $\tilde{\phi}_s$ during the voltage sweep even without any explicit variation in the actual T_e.

From the data shown in Fig. 5, typically we measure $\tilde{n}/n\gtrsim 0.3$ and $e\tilde{\phi}_f/T_e\cong 0.5$ using a probe near the swept T_e probe, each with an average frequency of $f\lesssim 200$ kHz.[17] Thus for a typical sweep of $dV=50$ V over $\cong 1\,\mu$sec used for the calculation of T_e (see Fig. 3), we have for the density dependent term in Eq. (13), $\Delta T_e'/T_e=(kT_e/e)d(\ln n)/dV=(kT_e/ne)(d\tilde{n}/dt)/(dV/dt)$. Taking a typical value for $d\tilde{n}/dt$ of $2\pi f\tilde{n}$, we obtain $\Delta T_e'/T_e\cong 3\%$, i.e., the *apparent* temperature fluctuation caused by expected variations in the density (causing variations in the apparent slope of the I vs V curve) is about 3% rms.

Similarly, for the potential dependent term in Eq. (13), taking $\tilde{\phi}_s\cong\tilde{\phi}_f$ (consistent with the tentative assumption that the actual $\tilde{T}_e\cong 0$), we have $\Delta T_e'/T_e\cong(d\tilde{\phi}_f/dt)(dt/dV)\cong 10\%$, i.e., the *apparent* temperature fluctuation caused by expected variations in space potential is about 10% rms.

Thus the combination of these two independent error sources gives a total uncertainty associated with Eq. (13) of $\Delta T_e'/T_e\cong 11\%$. This uncertainty was added to the individual uncertainty in the fit of each (I,V) sweep ($\cong 3\%$–5%) to produce the error bars shown in Fig. 4. This analysis implies that the observed variations in the apparent slope of the (I,V) curves of the $\lesssim 15\%$ rms were not significantly greater than the uncertainties in the determination of each T_e measurement, i.e., that the actual temperature fluctuation could not be resolved but was less than $\tilde{T}_e/T_e\cong 15\%$.

D. Possible improvements

The most obvious direction for improvement in this diagnostic method is to increase the sweeping frequency so that the background density and potential fluctuate negligibly over the effective sweep time. Considering the error analysis of Sec. III C, one would expect that an accuracy of $\cong 1\%$ in the T_e measurement could be obtained with a sweep frequency of about ten times the present value, i.e., $\cong 3$ MHz. This requires a considerable improvement in the driving amplifier if the probe current of $\gtrsim 1$ A is to be accommodated.

A more subtle improvement can be made by attempting to measure simultaneously the local $\tilde{n}$ and $\tilde{\phi}_f$ within the same region of fluctuating plasma in order to explicitly correct the time dependent signal from the swept probe for the variations. This was not attempted in the present context, mainly because the spatial correlation lengths of these fluctuations of 0.5–1.0 cm[10] were so short.

Along a similar line, one can form a compact multiprobe array of separate fixed-bias probes in order to reconstruct the (I,V) characteristic at each sampling time.[20] This was

attempted in the present case using an array of 12 probes mounted together in an array $\sim 5 \times 5$ mm in size. Although the average electron temperature determined from this array was consistent with that determined from the swept probe method, it was found that the correlation in $\tilde{n}$ among these probes was too low to assume that $\tilde{n}$ (or $\tilde{\phi}_f$) was constant across the array. Thus possible fluctuations in T_e were totally masked by spatial fluctuations in $\tilde{n}$ (consistent with the average spatial correlation lengths [10]).

IV. HEAT FLUXES IN THE EDGE REGIONS OF THE CALTECH TOKAMAK

The determination of the upper bound on the $\tilde{T}_e$ fluctuations, presented in Sec. III, together with previous measurements of the microturbulence in the edge regions,[7,10-11] allows a comparison of the relative magnitudes of the electron heat fluxes caused by various turbulent mechanisms. In this section the fluxes and diffusivities caused by microscopic fluctuations in both the electric and magnetic fields are compared.

A. Heat fluxes associated with $\tilde{E}_p$

In Sec. II, expressions for the anomalous electron heat losses associated with electrostatic fluctuations were given that are valid for the edge regions of the Caltech tokamak. These heat loss processes are (1) the heat transport resulting from the anomalous particle flux $(5/2)T_e\Gamma_x = (5/2)T_e c\langle \tilde{E}_y \tilde{n}\rangle/B$ [Eqs. (1) and (2)] and (2) the conductive heat flux $q_x \cong (5/2)nc\langle \tilde{E}_y \tilde{T}_e\rangle/B$ [Eq. (9), valid for isotropic pressure fluctuations]. The ratio of these two heat losses is

$$\frac{q_x}{\frac{5}{2}T_e\Gamma_x} \cong \frac{n\langle \tilde{T}_e \tilde{E}_y\rangle}{T_e\langle \tilde{n}\tilde{E}_y\rangle}. \tag{14}$$

The anomalous particle flux resulting from the density and electric field fluctuations has been measured directly in the edge regions of the Caltech tokamak by correlating probe measurements of $\tilde{n}$ and $\tilde{E}_y$.[7,10] The correlation can be expressed in the form

$$\langle \tilde{n}\tilde{E}_y\rangle = \int df\, C_{nE}(f)|\tilde{n}(f)|\,|\tilde{E}_y(f)|\cos\theta(f), \tag{15}$$

where $C_{nE}(f)$ is the coherence of the $\tilde{n}$ and $\tilde{E}_y$ probe signals over a small frequency range around f.[7,10] The results of the measurement of the particle flux were as follows: (1) the flux was mainly caused by large-amplitude, low-frequency fluctuations ($f \lesssim 100$ kHz); (2) the phase angle was such that $\cos\theta \cong 1$ for $f < 100$ kHz, and the coherence was $C_{nE}(f) \cong 0.2$–0.5 for $f < 100$ kHz. Thus one can write

$$\langle \tilde{n}\tilde{E}_y\rangle \cong (0.2 - 0.5)\,|\tilde{n}|\,|\tilde{E}_y|. \tag{16}$$

Using the measured upper bound on the electron temperature fluctuations and the measured correlation in Eq. (16), an upper bound can be placed on the ratio of the heat fluxes in Eq. (14). Using $\langle \tilde{T}_e\tilde{E}_y\rangle < |\tilde{T}_e|\,|\tilde{E}_y|$, and $|\tilde{T}_e/T_e| < 0.5|\tilde{n}/n|$ as measured, Eq. (14) yields

$$\frac{q_x}{\frac{5}{2}T_e\Gamma_x} < 0.5\,\frac{|\tilde{n}|\,|\tilde{E}_y|}{\langle \tilde{n}\tilde{E}_y\rangle} < 2. \tag{17}$$

Thus the measurements indicate that the electron heat flux caused by thermal conduction is at most about twice the heat flux resulting from the particle flux. Note that this is only an upper bound on the relative amount of electron heat loss by conduction. If the actual electron temperature fluctuations are significantly smaller than the upper bound of 15% or if the coherence of the electric field and electron temperature fluctuations is significantly less than 1 [i.e., if $\langle \tilde{T}_e\tilde{E}_y\rangle/|\tilde{T}_e|\,|\tilde{E}_y| \sim 0.2 - 0.5$ as found for the $\tilde{n}$ and $\tilde{E}_y$ correlation, Eq. (16)], then the heat flux carried by the thermal conduction would be significantly less than the heat flux caused by anomalous particle diffusion.

It should be noted that the measurements of the temperature fluctuations and particle fluxes were not made simultaneously, but the experimental conditions are quite similar. The temperature fluctuation measurement was made at the top of the torus, whereas the particle flux was measured at both the top and the outer edge with similar results. Also, density fluctuations were measured at the top, outside, and inside of the torus with similar results.[17] Thus, we have assumed that the turbulence and fluxes are poloidally symmetric.

Equation (17) indicates that the heat flux carried by the particle flux is comparable to or larger than the heat lost by conduction in the edge regions of this tokamak. Using the measured particle flux, this heat transport can be compared to the estimated global heat transport. The magnitude of the $\tilde{E}$-induced particle flux in the edge regions was measured to be $\Gamma_x(\tilde{E}) = c\langle \tilde{n}\tilde{E}_y\rangle/B \cong 1$–$2 \times 10^{17}\ \mathrm{cm}^{-2}\ \mathrm{sec}^{-1}$.[7,10] Taking $\Gamma_x \cong D\,dn/dx$ and using the measured density gradient, $dn/dx \sim 5 \times 10^{11}\ \mathrm{cm}^{-4}$ (within a factor of 2), one obtains the particle diffusion coefficient in the edge, $D(\tilde{E}) \sim (1-4) \times 10^5\ \mathrm{cm}^2/\mathrm{sec}$. This is somewhat larger than the global electron thermal diffusivity of $\chi_e \sim 0.5$–$1.0 \times 10^5\ \mathrm{cm}^2$ estimated from the measured global energy confinement time of 0.5–1.0 msec using the formula $\chi_e \sim a^2/4\tau_E$. Thus we conclude that the heat loss caused by the measured $\tilde{E}$-induced particle flux is an important energy loss mechanism in the edge regions of this tokamak. Moreover, it is of the correct magnitude to account for all of the electron energy loss in the edge region, although other electron energy loss processes, such as impurity radiation, charge exchange, and ionization, may also be present. Note that Taylor discharge cleaning was used for these discharges, and thus losses from impurity radiation should be relatively small.

Using Eq. (17), we can also put an upper limit on the ratio of the thermal and particle diffusivities associated with $\tilde{E}_y$, $\chi_e(\tilde{E})$, and $D(\tilde{E})$ in the edge regions. Since $q_x = n\chi_e(dT_e/dx)$, Eq. (17) yields

$$\frac{D(\tilde{E})}{\chi_e(\tilde{E})} > 0.2\,\frac{d\ln T_e/dx}{d\ln n/dx}.$$

Previous measurements in the edge regions of this tokamak[17] give $[d(\ln T)/dx]/[d(\ln n)/dx] \lesssim 1$, so we can conclude that $D(\tilde{E})$ is at least comparable to $\chi_e(\tilde{E})$ in the edge regions, but $\chi_e(\tilde{E})$ may still be larger.

B. Heat flux from magnetic fluctuations

Broadband microscopic magnetic fluctuations at a level $\tilde{B}_r/B \cong 2 \times 10^{-4}$ were measured in the edge regions of the

Caltech tokamak by Hedemann.[11] (For similar measurements in other tokamaks, see Ref. 1 and references therein.) The electron heat flux caused by these fluctuations can be estimated using theoretical models of the electron thermal conductivity resulting from stochastic magnetic field fluctuations (see, e.g., Refs. 21 and 1 and references therein.)

The model appropriate for Caltech parameters is the collisionless model of Rechester and Rosenbluth,[12] valid when the electron mean free path is longer than the parallel correlation length of the turbulence, L_0. Taking $L_0 \sim qR$, the Rechester–Rosenbluth model gives $\chi_e(\tilde{B}) \cong qRv_e(\tilde{B}_r/B)^2 \cong 2\times 10^3$ cm^2/sec, where $v_e (\cong 2\times 10^8$ cm/sec) is the electron thermal velocity for $T_e \cong 25$ eV as measured in the edge, $q(\cong 4)$ is the safety factor, and $R(=45$ cm) is the major radius. [If the mean free path were shorter than the correlation length L_0, the thermal diffusivity $\chi_e(\tilde{B})$ would be reduced.[12,21]] The resulting radial heat flux is given by $q_x(\tilde{B}) = n\chi_e(\tilde{B})(dT_e/dx)$, and the ratio of this heat flux to the radial heat loss by the measured particle flux is

$$\frac{q_x(\tilde{B})}{\frac{5}{2}T_e\Gamma_x(\tilde{E})} \sim \frac{\chi_e(\tilde{B})}{D(\tilde{E})}\frac{d\ln T_e/dx}{d\ln n/dx} < 10^{-2},$$

since $\chi_e(\tilde{B})/D(\tilde{E}) \sim 10^{-2}$ and $[d(\ln T)/dx]/[d(\ln n)/dx] \lesssim 1$ in the Caltech edge.[17] Thus, the heat flux caused by the microscopic magnetic fluctuations is negligible compared to the heat flux resulting from the $\tilde{E}$-induced particle flux in the edge regions (see also Ref. 18).

C. Estimate of neoclassical fluxes

For completeness, the neoclassical fluxes have also been estimated for the Caltech Research Tokamak using the Chang–Hinton formula for the ion neoclassical thermal diffusivity χ_i (Ref. 22). It was found that for core parameters ($T_i \cong 75$ eV, $r = 7$ cm, $R = 45$ cm, $n = 5\times 10^{12}$ cm^{-3}, $B = 3.5$ kG, $Z_{\text{eff}} \cong 1.5$), the diffusivity is $\chi_i \cong 2\times 10^4$ cm^2/sec; for edge parameters ($T_i \cong 30$ eV, $n \cong 10^{12}$ cm^{-3}, $r = 15$ cm), the diffusivity is $\chi_i \cong 10^4$ cm^2/sec. The neoclassical electron thermal diffusivity and the particle diffusion coefficient will be smaller by approximately $\sqrt{m_e/m_i}$. Thus the electron neoclassical thermal flux and the neoclassical particle flux are about two orders of magnitude smaller than the observed anomalous fluxes discussed in this section.

V. DISCUSSION

An upper limit has been placed on the magnitude of the electron temperature fluctuations $\tilde{T}_e$ in the edge regions of the Caltech Research Tokamak. This measurement, together with previous measurements of the edge fluctuations, allowed a unique comparison of the heat fluxes caused by various turbulent mechanisms. The measurements indicated that the heat loss associated with the measured turbulent particle flux resulting from $\tilde{n}$ and $\tilde{E}$ is as large as or larger than the loss via thermal conductivity caused by $\tilde{E}$ and $\tilde{T}_e$ fluctuations and about 100 times larger than the heat loss expected from the measured magnetic fluctuations $\tilde{B}_r$. The various assumptions involved in making these comparisons were discussed in Sec. IV.

The anomalous particle diffusion coefficient in the edge region, estimated from the measured $\tilde{E}$-induced particle flux, was shown to be comparable but somewhat larger than the global electron thermal diffusivity estimated from the measured global energy confinement time. Thus the heat loss associated with this particle flux is a significant energy loss mechanism in the edge region. In fact, the heat loss carried out by the measured anomalous particle flux seems large enough to account for all the electron heat loss at the edge. Whether or not it is the only important electron energy loss process in the edge region remains an open question.

Another implication of the $\tilde{T}_e$ measurement relates to the diagnostic interpretation of measured fluctuations in the ion saturation current. Generally, for the edge regions of this tokamak, it is assumed that the electron temperature fluctuations are negligible and the fluctuations in $I_{i,\text{sat}} \sim nT_e^{-1/2}$ are assumed to be proportional to the density fluctuations. This assumption in now better justified since for $|T_e/T_e| < 15\%$ when $|\tilde{n}/n| \lesssim 30\%$, the temperature fluctuations produce at most a 25% effect on $\tilde{I}_{i,\text{sat}}/I_{i,\text{sat}}$. On the other hand, the usual assumption concerning the relation of fluctuations in the floating and space potentials, $\tilde{\phi}_s = \tilde{\phi}_f$, can *not* be justified at present since if $|\tilde{T}_e/T_e| \cong 15\%$ and if $\tilde{\phi}_s \cong \tilde{\phi}_f + 3\tilde{T}_e$ [see Eq. (11)], then the possible $\tilde{T}_e \cong 2$ eV can contribute significantly to the observed $\tilde{\phi}_f \lesssim 10$ V.

The measured bound of 15% for the relative temperature fluctuations was found when simultaneously $\tilde{n}$ and $\tilde{\phi}$ fluctuations were 30%–50%. This measured ratio, $|\tilde{T}_e/T_e| < |\tilde{n}/n|$, is consistent with several theoretical models of edge fluctuations. A model of edge turbulence caused by resistive MHD rippling modes[23] predicted a temperature fluctuation level of $\tilde{T}_e/T_e \cong 5\%$ for parameters typical of the edge of the Macrotor tokamak[24]; the corresponding density fluctuation level was estimated to be $\tilde{n}/n \cong 20\%$.[23] Linear models of collisional drift and drift-rippling modes, investigated by Horton[13] and Hassam and Drake,[25] respectively, are also consistent with $|\tilde{T}_e/T_e| < |\tilde{n}/n|$ (for comparable density and temperature gradient scale lengths) because of the importance of classical parallel electron thermal conductivity in limiting $\tilde{T}_e$. Linear models of collisionless and trapped electron drift waves would also generally predict $\tilde{T}_e/T_e \sim (\gamma/\omega)\,\tilde{n}/n \ll \tilde{n}/n$, where γ is the growth rate and ω is the frequency of the drift wave. Note, however, that $\tilde{T}_e/T_e < \tilde{n}/n$ does not, in general, imply that the transport from convection is larger than the transport from conduction since it is the correlation as well as the magnitude of the fluctuations that determine the resulting transport. For example, quasilinear calculations of transport from dissipative trapped electron instabilities (see, e.g., Horton and Estes[26]) indicated that the thermal conduction losses can be significantly larger (up to five times) than convective losses even though for this drift mode $\tilde{T}_e/T_e \sim (\gamma/\omega)\,\tilde{n}/n$. This is because the necessary correlations are of comparable magnitude, i.e.,

$$\langle \tilde{n}\tilde{E}_y\rangle T_e \sim (\gamma/\omega)|\tilde{n}|\,|\tilde{E}_y|T_e \sim n\langle \tilde{T}_e\tilde{E}_y\rangle \sim n|\tilde{T}_e|\,|\tilde{E}_y|.$$

One can make a rough estimate of the temperature fluctuations that should accompany magnetic fluctuations of the measured level, $\tilde{B}_r/B \cong 2\times 10^{-4}$ (Ref. 11). Assuming the

electrons have infinite parallel electron thermal conductivity (see, e.g., Ref. 13), one obtains

$$\frac{\tilde{T}_e}{T_e} \cong \frac{\tilde{B}_r}{B_T}\frac{1}{k_\parallel L_T},$$

where $L_T^{-1} = d(\ln T)/dx$ is the temperature gradient scale length. For Caltech edge parameters ($k_\parallel^{-1} \sim qR \sim 200$ cm, $L_T \sim 2$ cm), one obtains $\tilde{T}_e/T_e \sim 2\times 10^{-2}$, well below the measured upper limit (Sec. III).

The fact that the heat conduction from the magnetic fluctuations was found to be unimportant in edge regions of the Caltech tokamak does not indicate that magnetic fluctuations will not be important in other, higher-β situations since the magnetic fluctuations are generally expected to increase with β. For instance, the approximate level of magnetic fluctuations from drift wave turbulence found by Waltz[27] is $|\tilde{B}_r/B| \sim (q\beta/2)|\tilde{n}/n|$, where β is the toroidal β; in Ref. 27, this estimate is shown to fit the measured ratio on the Macrotor tokamak. The resulting electron thermal transport can be compared to an estimate of the transport from electrostatic drift waves to give a rough indication of the β at which transport from magnetic fluctuations will be significant. Using the Rechester and Rosenbluth collisionless model of the electron thermal diffusivity with the above estimate for $\tilde{B}_r$, one obtains $\chi(\tilde{B}) \sim v_{te} q^3 R (\beta/2)^2 (\tilde{n}/n)^2$. The conductivity from electrostatic drift waves can be estimated as $\chi(\tilde{E}) \sim k\rho_s(\gamma/\omega)c_s L_n(\tilde{n}/n)^2$, where L_n is the density gradient scale length, k is the perpendicular wavenumber, ρ_s is the ion gyroradius with the electron temperature, and c_s is the sound speed. Taking $(\gamma/\omega) \sim 0.1$ and $k\rho_s \sim (0.3\text{–}1.0)$, one obtains $\chi(\tilde{B})/\chi(\tilde{E}) \sim (2\text{–}8)\times(q\beta)^2(qR/L_n)\sqrt{(m_i/m_e)}$. Thus, these estimates suggest that for $\beta \gtrsim (0.04\text{–}0.1)L_n/(q^3R) \sim 1\%$, the thermal conduction from magnetic fluctuations might be expected to dominate over the electrostatic transport.

The Caltech tokamak is the only experiment to date in which the turbulence-induced heat flux can be studied in such detail. However, the edge turbulence observed in the Caltech tokamak is not unique; similar edge turbulence has been observed and studied using both scattering and probe techniques in other tokamaks, both large and small (see Ref. 1 and references therein). For instance, in the Alcator C tokamak, edge density fluctuations at a level $\tilde{n}/n \sim 40\%$ have recently been studied.[3]

Since edges of many other tokamaks, both large and small, have similar parameters and turbulence, the heat flux from the turbulence-induced particle flux may be important in these experiments as well. Comparison of results from PDX in the H and L modes gives indirect evidence that particle transport leads to a significant electron heat loss: in the H mode, the edge particle confinement is better and the edge electron temperature higher than in L mode discharges.[28] If the energy loss associated with the particle flux is an important energy loss mechanism in larger tokamaks, it might be possible to lower this heat loss at the edge by lowering the particle transport associated with edge turbulence, for example, through modifying local density gradients via changes in the fueling.

ACKNOWLEDGMENTS

One of the authors (P. C. L.) would like to thank Paul Bellan and Wendell Horton for helpful discussions.

This work was supported by the Office of Fusion Energy of the U. S. Department of Energy.

APPENDIX: DERIVATION OF EXPRESSIONS FOR PARTICLE AND HEAT FLUXES RESULTING FROM LOW-FREQUENCY, ELECTROSTATIC FLUCTUATIONS

Particle and heat fluxes caused by low-frequency, electrostatic fluctuations have been calculated by several authors,[13–16] generally for the case of drift wave fluctuations. Here, we briefly review the calculation for the case of arbitrary low-frequency, electrostatic fluctuations.

In the presence of low-frequency ($\omega \ll \omega_{ci}$), electrostatic ($\tilde{B} \cong 0$) turbulence, the effect of the fluctuations on the microscopic evolution of the plasma is calculated by separating the distribution function and the electric field into average or macroscopic parts, which evolve on a slow, transport time scale, and microscopic, rapidly varying parts associated with the microturbulence, i.e.,

$$F = \langle F \rangle + \tilde{F}$$

and

$$\mathbf{E} = \langle \mathbf{E} \rangle + \tilde{\mathbf{E}},$$

where $\langle\ \rangle$ denotes a time average over the fluctuation time scale so that $\langle \tilde{F} \rangle = \langle \tilde{\mathbf{E}} \rangle = 0$ and $\langle F \rangle$ and $\langle \mathbf{E} \rangle$ are macroscopic quantities. Averaging the Vlasov equation over the fluctuation time scale yields

$$\left[\frac{\partial}{\partial t} + \mathbf{v}\cdot\frac{\partial}{\partial \mathbf{x}} + \frac{q}{m}\left(\langle \mathbf{E} \rangle + \frac{\mathbf{v}\times\mathbf{B}}{c}\right)\cdot\frac{\partial}{\partial \mathbf{v}}\right]\langle F \rangle = \frac{-q}{m}\left\langle \tilde{\mathbf{E}}\cdot\frac{\partial \tilde{F}}{\partial \mathbf{v}}\right\rangle + \langle C(F) \rangle, \tag{A1}$$

where the effects of the electrostatic turbulence are contained in the correlation $\langle \tilde{\mathbf{E}}\cdot\partial\tilde{F}/\partial\mathbf{v}\rangle$ and $\langle C(F)\rangle$ is the operator for all the classical, collisional processes. The equations for the evolution of the macroscopic plasma variables in the presence of the classical (and neoclassical) and turbulent processes are obtained from the velocity moments of Eq. (A1). In the derivation below, contributions from the classical processes will not be included and slab geometry will be used (cf. Sec. II).

The first two even moments of Eq. (A1), in which the terms involving the magnetic field vanish, yield the equations for the evolution of the density and temperature,

$$\frac{\partial}{\partial t}n + \frac{\partial}{\partial x}nV_x = 0, \tag{A2}$$

$$\frac{3}{2}\frac{\partial}{\partial t}nT + \frac{\partial}{\partial x}\left(\frac{5}{2}TnV_x + q_x\right) = V_x\frac{\partial nT}{\partial x} + qn\langle \tilde{\mathbf{V}}\cdot\tilde{\mathbf{E}}\rangle.$$

The radial particle flux is $\Gamma_x = nV_x$ and the heat transported by this particle flux is $(5/2)T\Gamma_x$. The remainder of the heat flux, q_x, generally referred to as the thermal conduction flux, represents the heat transport that takes place without any corresponding particle transport.

The $\hat{y}$ components of the first two odd moments of Eq. (A1) are

$$\frac{\partial}{\partial t} nV_y + \frac{\partial}{\partial x} nV_x V_y = -\frac{q}{m} n \frac{V_x B_z}{c} + \frac{q}{m} \langle \tilde{n} \tilde{E}_y \rangle, \tag{A3}$$

$$\frac{\partial}{\partial t} W_y + \frac{\partial}{\partial x} H_{xy} = -\frac{q}{m} \frac{W_x B_z}{c} + \frac{q}{m} \langle \tilde{\epsilon} \tilde{E}_y \rangle + \frac{q}{m} \times \left\langle \int d\mathbf{v}\, m v_y \mathbf{v} \cdot \tilde{\mathbf{E}} \tilde{F} \right\rangle, \tag{A4}$$

where $H_{xy} = \int d\mathbf{v}\, v_x v_y (mv^2/2) \langle F \rangle$. The definitions of the other macroscopic (fluid) and microscopic (fluctuating) quantities are given in Sec. II, Eqs. (3)–(6), and the relation between the total radial energy flux W_x and the conductive heat flux q_x is given in Eq. (7). The set of equations [Eqs. (A2)–(A4)] is closed using the standard method: the time variation of the macroscopic quantities is assumed to be slow compared to gyrotimes and the characteristic length for spatial variation of the macroscopic quantities is assumed to be long compared to the gyroradius, i.e., $(1/\omega_c)\partial(\ln F)/\partial t \ll 1$ and $(v/\omega_c)\partial(\ln F)/\partial x = \rho \partial(\ln F)/\partial x \ll 1$, where $\omega_c = qB/mc$ is the gyrofrequency and $\rho = v/\omega_c$ is the gyroradius. With these orderings, the terms on the left-hand sides of Eqs. (A3) and (A4) can be neglected, yielding closed expressions for the turbulent fluxes Γ_x and W_x in terms of moments of the "turbulent" collision operator $\langle \tilde{\mathbf{E}} \cdot \partial \tilde{F}/\partial \mathbf{v} \rangle$: Eq. (A3) yields the standard expression for the particle flux Γ_x caused by the electrostatic turbulence given in Eq. (1), and Eq. (A4) yields the expression for the energy flux W_x caused by the electrostatic turbulence given in Eq. (5).

[1] P. C. Liewer, Nucl. Fusion **25**, 543 (1985).
[2] E. Mazzucato, Phys. Rev. Lett. **48**, 1828 (1982).
[3] R. E. Slusher and C. M. Surko, Phys. Rev. Lett. **40**, 400 (1978); R. L. Watterson, R. E. Slusher, and C. M. Surko, Phys. Fluids **28**, 2857 (1985).
[4] Equipe TFR, Plasma Phys. **25**, 641 (1983).
[5] R. E. Slusher, C. M. Surko, J. F. Valley, T. Crowley, E. Mazzucato, and K. McGuire, Phys. Rev. Lett. **53**, 667 (1984).
[6] D. L. Brower, W. A. Peebles, N. C. Luhman, and R. L. Savage, Phys. Rev. Lett. **54**, 689 (1985).
[7] S. J. Zweben, P. C. Liewer, and R. W. Gould, J. Nucl. Mater. **111&112**, 39 (1982).
[8] S. J. Levinson, J. M. Beall, E. J. Powers, and R. D. Bengston, Nucl. Fusion **24**, 527 (1984).
[9] Ch. P. Ritz, R. D. Bengston, S. J. Levinson, and E. J. Powers, Phys. Fluids **27**, 2956 (1984).
[10] S. J. Zweben and R. W. Gould, Nucl. Fusion **25**, 171 (1985).
[11] M. A. Hedemann, Ph.D. thesis, California Institute of Technology, 1981.
[12] A. B. Rechester, and M. N. Rosenbluth, Phys. Rev. Lett. **40**, 38 (1978).
[13] W. Horton in *Basic Plasma Physics*, edited by A. A. Galeev and R. N. Sudan (North-Holland, Amsterdam, 1985), Vol. II, p. 383.
[14] D. F. Düchs, D. W. Post, and P. H. Rutherford, Nucl. Fusion **7**, 565 (1977).
[15] N. A. Krall and J. B. McBride, Nucl. Fusion **7**, 713 (1977).
[16] W. Manheimer and I. Cook, Comments Plasma Phys. **5**, 5 (1979).
[17] S. J. Zweben and R. W. Gould, Nucl. Fusion **23**, 1625 (1983).
[18] S. J. Zweben and R. J. Taylor, Nucl. Fusion **3**, 513 (1983).
[19] F. F. Chen, in *Plasma Diagnostic Techniques*, edited by R.H. Huddlestone, and S. L. Leonard (Academic, New York, 1975), p. 113.
[20] N. Wild, R. Stenzel, and W. Gekelman, Rev. Sci. Instrum. **54**, 935 (1983).
[21] J. A. Krommes, C. Oberman, and R. G. Kleva, J. Plasma Phys. **30**, 11 (1983).
[22] C. S. Chang and F. L. Hinton, Phys. Fluids **25**, 1493 (1982).
[23] L. Garcia, P. H. Diamond, B. A. Carreras, and J. M. Callen, Phys. Fluids **28**, 2147 (1985).
[24] S. J. Zweben and R. J. Taylor, Nucl. Fusion **23**, 193 (1981).
[25] A. B. Hassam and J. F. Drake, Phys. Fluids **26**, 133 (1983).
[26] W. Horton and R. D. Estes, Nucl. Fusion **9**, 203 (1979).
[27] R. E. Waltz, Phys. Fluids **28**, 577 (1985).
[28] S. M. Kaye, J. Nucl. Mater. **121**, 115 (1984).